Generation and evolution of two-dimensional dark spatial solitons

S. Baluschev, A. Dreischuh, I. Velchev, and S. Dinev
Sofia University, Faculty of Physics, 5 J. Bourchier Boulevard, BG-1126 Sofia, Bulgaria

O. Marazov
Spectronika Ltd., P.O. Box 16, BG-1336 Sofia, Bulgaria
(Received 20 December 1994; revised manuscript received 22 June 1995)

In this paper we demonstrate numerical and experimental results on the evolution characteristics of two-dimensional even and odd dark spatial solitons. Two-dimensional even dark spatial solitons are experimentally generated and investigated.

PACS number(s): 42.70.Nq, 42.50.Rh

I. INTRODUCTION

Generally, the nonlinear evolution of a beam or pulse should be described by the (3+1)-dimensional nonlinear Schrödinger equation (NLSE) [1] with three transverse dimensions: two spatial and time. The realistic modeling of the cw-beam spatial self-action requires the (2+1)-dimensional NLSE to be solved [2]. There are some specific cases, where the dimensionality could be reduced to (1+1): temporal evolution of a short pulse in single-mode optical waveguide [3], and evolution of the transverse profile of a cw elliptical beam in a planar waveguide [4]. The relatively simplified beam-pulse evolution results from the compensation of the optical beam diffraction by the total internal reflection (linear process).

The optical solitons form a specific class of beam-pulses for which the diffraction or group-velocity dispersion (GVD), respectively, is compensated by the medium nonlinearity [5,6]. The dark optical solitons could be characterized as localized dips superimposed upon a background beam-pulse. During the last several years, the generation and evolution of dark spatial solitons has been analyzed in one spatial dimension mainly. Recently, the influence of the two-dimensional (2D) background of a finite extent on the evolution of 1D even dark spatial solitons has been studied in [7]. The first theoretical analysis on the existence of stable 2D self-supported beams [8] was followed by the experimental generation of 2D odd dark spatial solitons (optical vortex solitons) [9–11]. They could be characterized as dark beams with on-axis 2π helical phase ramps [12] imposed on high-intensity background beams. Two publications of Kivshar and Yang discuss the existence, the propagation characteristics, and the perturbation stability of ring dark solitons [1,13]. In a recent experiment, these formations were generated and investigated [14]. From an interferogram analysis, pairs of diametrical phase shifts across each ring were retrieved [14].

In the following we will present additional evidence that two-dimensional odd and even dark optical solitons [(ODSS), (EDSS)] do exist. Odd and even initial conditions of the NLSE will be considered. Extensive numerical simulations in two dimensions and comparisons with the propagation characteristics of the 1D dark spatial solitons (soliton stripes [15,16]) are presented, demonstrating a well-pronounced soliton evolution of the input dark formations. 2D even dark spatial solitons are experimentally generated and investigated.

II. TWO-DIMENSIONAL ODD DARK SPATIAL SOLITONS

Analytically, the 2D spatial evolution of an angularly symmetrical laser beam along a nonlinear medium is described by the (2+1)-dimensional NLSE [2]:

$$i\frac{\partial}{\partial z}E+\beta\left[\frac{\partial^2}{\partial x^2}+\frac{\partial^2}{\partial y^2}\right]E+kn_2|E|^2E=0\ , \tag{1}$$

where z is the longitudinal coordinate, x and y are the two transverse coordinates, $k=2\pi/\lambda$ is a wave number corresponding to the pulse wavelength λ, and $\beta=(2k)^{-1}$ accounts for the spatial beam diffraction in both transverse dimensions. The nonlinear term in Eq. (1) involves the intensity-dependent medium refractive-index correction $n_2|E|^2$. Depending on the sign of n_2, the nonlinearity can enhance (at $n_2<0$) or compensate (at $n_2>0$), at least partially, for the beam diffraction.

Let us consider briefly the physical picture in one transverse spatial dimension. The bright spatial optical solitons result from the balanced counteraction of the one-dimensional beam diffraction and self-focusing along a nonlinear medium. The usual 1D analysis assumes a continuous wave (cw), or quasi-cw input beams of high ellipticities and the basic NLSE has the form [4,6]

$$i\frac{\partial}{\partial z}E+\beta\frac{\partial^2}{\partial x^2}E+kn_2|E|^2E=0\ . \tag{2}$$

The diffraction tends always to spread out the beam in space (i.e., the diffraction coefficient β is always a positive one). Therefore, bright spatial solitons (in one dimension) could exist in self-focusing ($n_2>0$) media only [4,6]. Dark spatial solitons could be formed in self-defocusing ($n_2<0$) media [15,16]. The fundamental black spatial

soliton is described by an antisymmetric function of space (hyperbolic tangent), which causes an abrupt phase shift (phase step) of π at its center. This soliton is denoted as an odd dark spatial soliton, in contrast to the even dark (spatial) solitons, which do not have an initial phase shift. As a consequence, independent from the background intensities, the last ones split at least into two odd dark solitons with a reduced contrast ("gray" solitons), each one with its own phase shift (less than π) [17,18]. It has been recently shown that for a certain phase shift larger than π, two soliton solutions with different contrast do exist in the 1D case [19].

Let us concentrate our attention on the 2D odd input dark formations. In the first experiments they are generated utilizing the modulational instability of soliton stripes against long-period modulation [9,10]. In order to ensure adequate and controllable initial conditions for the formation of a 2D ODSS, a 2D spatial phase distribution, shown on Fig. 1, should be imposed on a plane wave front. Characteristic of this phase distribution [12] is a π phase shift (localized at the soliton center) in each radial direction. Practically, it could be achieved with an experimental scheme, similar to those depicted on Fig. 2(a). The laser source provides an initial beam, serving later as a background beam for the 2D ODSS. The 2D phase distribution required (Fig. 1) can be achieved after a properly constructed phase mask (PM). Further, the phase modulated background beam should be amplitude modulated by passing through a mask (AM). For the formation of a 2D ODSS, this mask should be circularly symmetric, on-axially aligned with respect to the background phase distribution, and its transmission profile should approach as close as possible the 2D ODSS shape. A charge-coupled device (CCD) camera and a personal computer (PC) combined with filter sets (F1, F2) should form the data acquisition and recording equipment.

The construction of the PM is a specific problem. In Fig. 2(b), one possible experimental configuration is sketched. A flat topped control beam should be intensity modulated passing through an AM with a 2D transmission distribution shown on the right-hand side of Fig. 2(b). Within a thin nonlinear medium (NLM) of a spatially localized response, the amplitude modulation of the control beam should yield the desired phase modulation of the background beam. Thereafter, the control beam should be removed [the dashed box on Fig. 2(b)]. The exact radial π jump could be achieved by adjusting the intensity of the control beam. As a first step a circular gradient neutral density disk could play the role of an AM [in Fig. 2(b)].

As mentioned, the aim of the present work is to provide additional evidences that two-dimensional dark optical solitons do exist. In the absence of exact analytical and approximate numerical results, we assumed a 2D dark beam of the form (written in cylindrical coordinates)

$$E(r,\varphi,z=0)=A_0B(r)\tanh(r/r_0)\exp[i\phi(r,\varphi)],$$
$$r=(x^2+y^2)^{1/2} \tag{3}$$

with a phase distribution

$$\phi(r,\varphi)=m\varphi, \quad \varphi\in(0,2\pi) \tag{4}$$

and a background profile

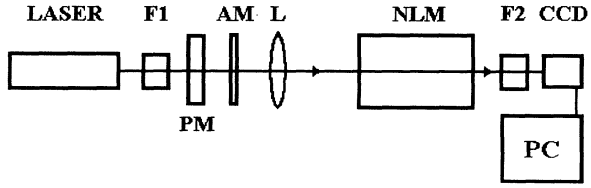

a)

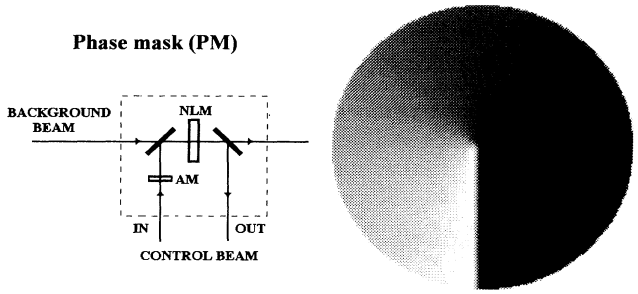

b)

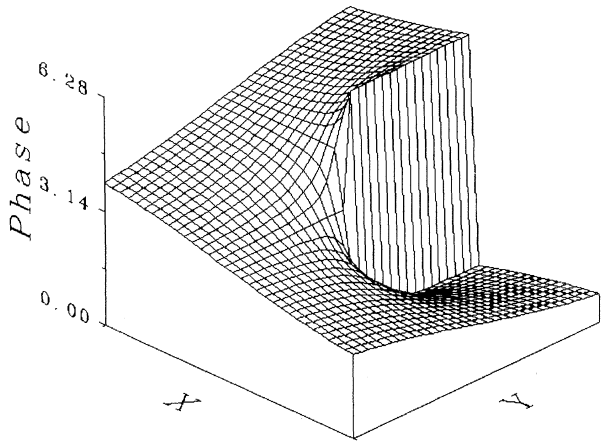

FIG. 1. Numerically generated phase distribution for obtaining a π-phase jump in an arbitrary radial direction.

FIG. 2. (a) Experimental scheme, corresponding to the numerical simulations. ($F1$, $F2$ are the filter sets; NLM is the self-defocusing nonlinear medium; AM is the amplitude mask for obtaining a 2D dip on the background; CCD denotes the camera and PC is the personal computer.) The PM should generate the desired radial π jump. (b) Possible scheme for achieving the appropriate background phase distribution. NLM denotes the thin nonlinear medium; the amplitude mask (AM) transmission (gray-scale coded) is plotted too.

$$B(r)=\exp\{-(r/[15r_0])^{16}\} \quad (5)$$

at the entrance face of the self-defocusing ($n_2<0$) nonlinear medium. In Eqs. (3)–(5), r and φ are radial and azimuthal coordinates, and m is an odd number. This distribution, predicted rather intuitively by adding a rotational symmetry to the transverse phase distribution of a 1D odd dark soliton [20], was proven numerically to be adequate in two spatial dimensions. We analyzed numerically the cw evolution of an initial (at $z=0$) intensity dip described by Eqs. (3) and (4) by solving Eq. (1). The numerical procedure used is a 2D generalization of the beam propagation method, based on split-step Fourier method [21].

Figure 3 shows a radial cross section of the input ($z=0$) 2D dark odd formation (curve a). The solid curve (b) represents the dark-beam shape at $Z=5L_{\rm nl}$, where $L_{\rm nl}=(kn_2|A_0|^2)^{-1}$ is the background nonlinear length [21]. This distribution, formed approximately at $Z=1.5L_{\rm nl}$, remains stable in the absence of a dip-to-background interaction (up to $Z=10L_{\rm nl}$ in our simulations). For comparison curve (c) shows the corresponding profile (at $Z=5L_{\rm nl}$) of an initial 1D odd dark beam (odd dark soliton stripe). It should be pointed out, that the shape of the resulting 2D dark formation closely reproduces the initial profile, given by Eq. (3). The smoother wings indicate that the input 2D hyperbolic tangent profile (assumed in 2D) slightly differs from the exact one for the 1D case. In order to explain qualitatively this behavior, we analyzed the NLSE [Eq. (1)], written in cylindrical coordinates, and searched for a partial solution of the form

$$E(r,\varphi,z)=A_0R(r)\exp(i\varphi)\exp(i\mu z)\ , \quad (6a)$$

where $\exp(i\varphi)$ corresponds to the phase distribution proposed [Fig. 1 and Eq. (4)]. The radial intensity distribution $R(r)$ was found in the form

$$R(r)\sim r\tanh(A_0r/\sqrt{2})W(r)\ , \quad (6b)$$

where $W(r)$ accounts for the singularities of the NLSE at $r=0$ and at infinity. The function $W(r)$ was found to tend to $1/r$ at $r\to\infty$ with lower values. Therefore, the intensity in the 2D ODSS wings should approach slower the background intensity, as compared to the hyperbolic-tangent profile assumed. Nevertheless, the hyperbolic-tangent seems a reasonable approximation for a 2D ODSS. It is interesting to note that the background intensity required for obtaining a 2D ODSS is $\sqrt{2}$ times higher than the respective value in the 1D case if equal

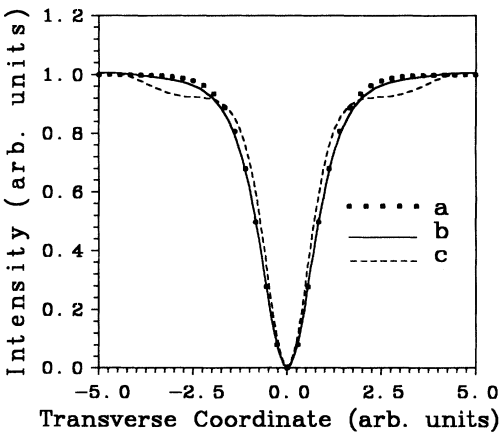

FIG. 3. Radial cross section of the input 2D dark odd formation (a) and fundamental 2D ODSS at $Z=5L_{\rm nl}$ (b). Curve (c) is a profile of an initial 1D odd dark beam at the same Z and background intensity.

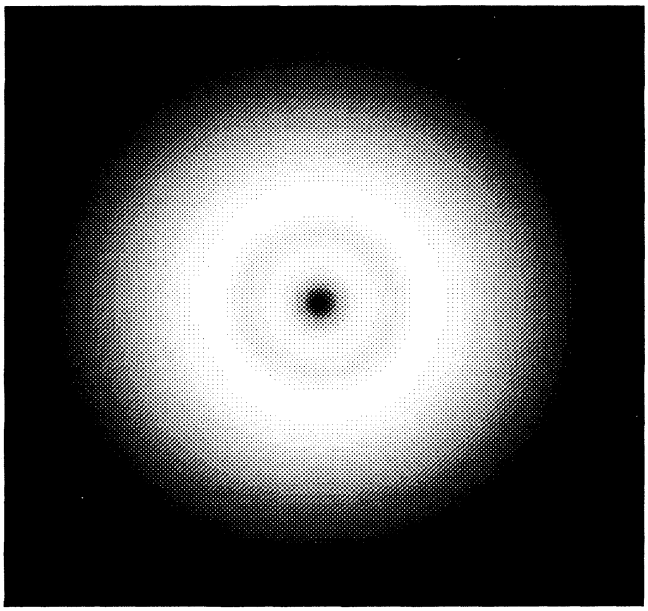

a)

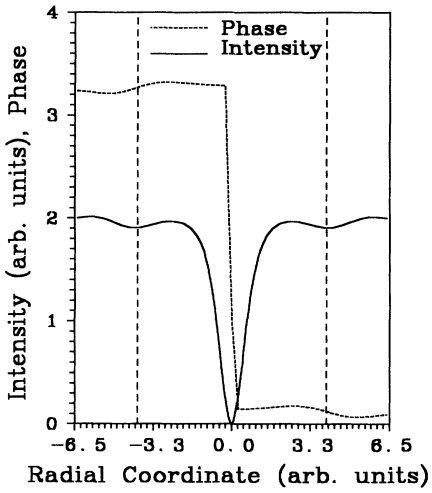

(b)

FIG. 4. Gray-scale image of the output 2D odd dark formation with $A_0=2.1$ at $Z=10L_{\rm nl}$ (a) and the corresponding radial intensity and phase distributions (b).

dark-beam diameters are assumed. This was mentioned for the first time in [9] [comment after Eq. (2)]. Physically, this numerical result could be attributed to the higher diffraction in two spatial dimensions as compared to the diffraction in one dimension. As seen from curve (c) on Fig. 3, the excessive "lack of energy" of the 1D input dark formation leads to the formation of a fundamental 1D ODSS and a diverging pair of 1D "gray" solitons. This behavior is consistent with the results of other authors in the one-dimensional case. Exceeding the background intensity for the fundamental 2D ODSS results in an evolution of the input single odd dark formation into an on-axis fundamental 2D ODSS and a diverging (along the nonlinear medium) "gray" ring. It corresponds to a dark soliton pair in the 1D case. The output 2D intensity distribution is demonstrated in Fig. 4(a) at $Z=10L_{\rm nl}$. The phase portrait [Fig. 4(b)] shows the undistorted π jump of the fundamental 2D ODSS and the smoother and of reduced amplitudes phase shifts across the gray ring. This behavior, known for the 1D odd dark solitons [20] strongly supports the statement, that the central dark beam is a 2D ODSS with a modulation depth of unity. However, the transverse spreading of the dark ring along the medium is accompanied with a 2D energy redistribution and with a decrease of the contrast. Consequently, the gray two-dimensional soliton ring is not a soliton formation itself, but it has a solitonlike evolution [1,13,14] and should be denoted as a ring dark soliton generated from a 2D odd dark soliton. In our opinion, these results confirm the statement, that 2D ODSS (optical vortex solitons) in bulk self-defocusing nonlinear media exist as "black" odd solitons only.

III. TWO-DIMENSIONAL EVEN DARK SPATIAL SOLITONS

As a second step we modeled numerically and observed experimentally the evolution of 2D even dark formations generated from even initial conditions (i.e., with an initial amplitude modulation only). The initial conditions in our numerical simulations are described by Eq. (3) with $\Phi=$const. The experiment performed was based on an arrangement, similar to those on Fig. 2(a). A 2D AM was illuminated with a laser beam prior to the NLM (ethanol slightly dyed in red). No PM was used in this case. Two filter sets ($F1$ and $F2$) were involved to control the background intensity and to prevent the CCD-camera saturation, respectively. A lens was used to image the AM on the entrance of the nonlinear medium. For the purpose of a comparative experimental analysis, the masks consisted of metal film dots and stripes (produced photolitographically) of equal diameters/widths ranging from 50 to 250 μm. A copper-vapor laser source ($P=4$ W) was used to produce the background beam, required for a background self-defocusing in a thermal nonlinear medium. This technique has been used for generating 1D dark spatial solitons [15,16,22]. The output dark formations were detected and recorded by a CCD camera and a frame grabber.

Increasing the intensity, four characteristic pictures (Fig. 5) were obtained from the calculations 5(a)–5(d) and during the experiment 5(e)–5(h). A Poisson spot is clearly seen on Fig. 5(a) as a result of a free-space propagation of the initial 2D even dark formation at one diffraction length. At higher intensity the medium nonlinearity compensates for the initial diffraction [Fig. 5(b)]. The background intensity enhancement yields a formation of a dark soliton ring [Fig. 5(c)], which is a 2D analog of the diverging 1D dark soliton pair. Qualitatively similar to the 1D case, the radial phase distribution exhibits two phase shifts (in opposite directions). The intensity within the ring was found to be higher than the background one, in contrast to the 1D case, where they are approximately equal. Figure 5(d) shows an initial stage of a second dark ring formation at a higher intensity.

Qualitatively, the same dark-beam evolution stages are

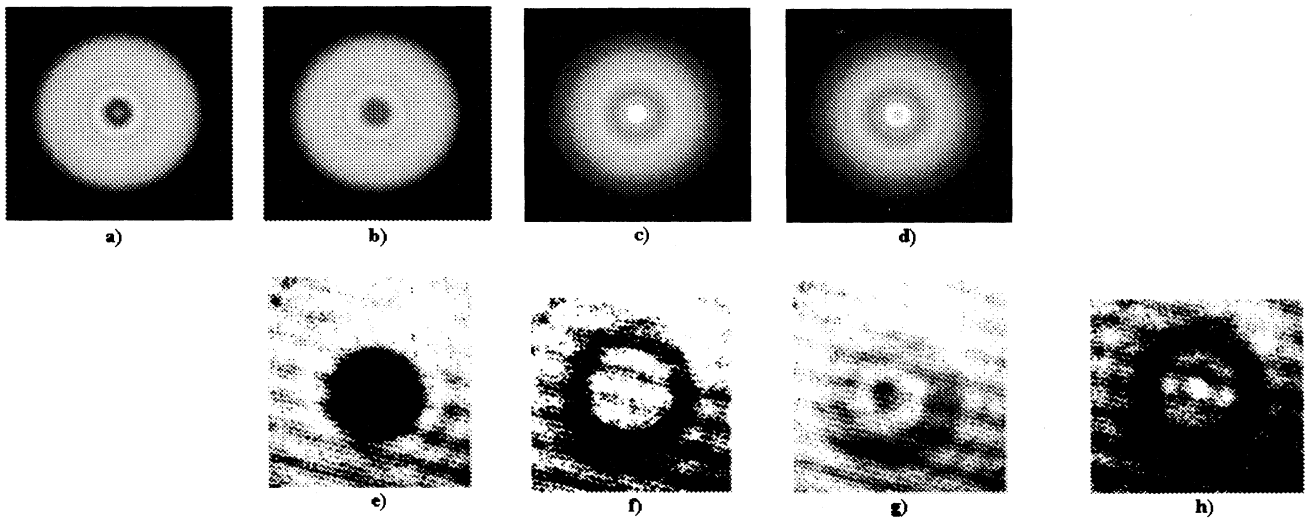

FIG. 5. Characteristic evolution stages of a 2D EDSS [(a)–(d) are numerically simulated; (e)–(h) are experimentally obtained]: Poisson spot at dark-beam center (a); diffraction compensated by the nonlinearity (b) and (e); first dark soliton ring (c) and (f); initial stage of the second dark soliton ring formation (d) and (g); two dark soliton rings (h).

observed experimentally (Figs. 5(e)–5(h)). The 2D dark formation from Fig. 5(e) is a result of a diffraction compensation by the nonlinearity. A dark (gray) ring with a central intensity higher than the background level [Fig. 5(f)] was observed too. Unfortunately, it was difficult to distinguish a small-scale interference dislocation (originating from the phase shift) across the dark soliton ring in this experiment. A pair of opposite phase shifts across the ring was measured in a separate experiment by using the four-frame technique for interferogram analysis [14]. Figure 5(g) corresponds qualitatively to the numerically generated Fig. 5(d). The loss of contrast is a result of the 2D redistribution of the "lack of energy" within the diverging (along the nonlinear medium and thereafter) dark ring. In order to avoid the CCD camera saturation, Fig. 5(h) was recorded with a neutral density filter, placed directly in front of the CCD array. This figure indicates the formation of two dark soliton rings. The interference lines in Fig. 5(e)–5(h) resulted from the NLM quvette input and output faces and were difficult to avoid. Nevertheless the figures are indicative for the modulation stability of the evolution of 2D EDSS.

Our comparative numerical simulations in one and two spatial dimensions show that the initial diffraction compensation and the subsequent spatial splitting take place earlier (i.e., at shorter distances in the nonlinear medium) for the 2D even input dark formations as compared to the 1D dark ones.

The intensity dependencies demonstrated above do not guarantee that the 2D dark formations observed are 2D EDSS. Strong evidence of the soliton nature is the transverse velocity λ_n of the dark spatial soliton pairs. In our experiment as well as in the works of other authors in the one-dimensional case, a lens images the amplitude masks on the entrance of the nonlinear medium. Therefore, an initial diffraction wave-front perturbation is present. Under the same initial conditions, we modeled the evolution along the nonlinear medium of 1D and 2D dark formations with (over one diffraction length) and without initial diffraction. The results indicated that there is no strong dependence of the transverse velocity on the initial diffraction. As shown in [1], the radial velocity of the ring dark soliton is a function of its radius.

The EDSS transverse velocity λ_n is defined in connection with the divergence angle θ between the two gray

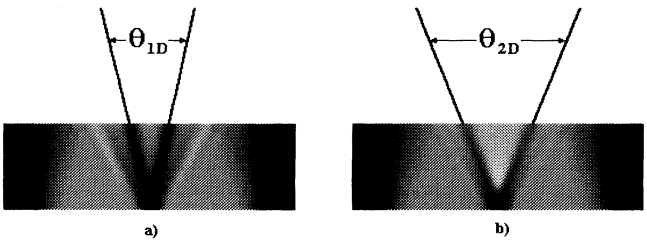

FIG. 6. Evolution of the transverse intensity distribution (as a sequence of radial slices) along the nonlinear medium. (a) 1D case; (b) 2D case.

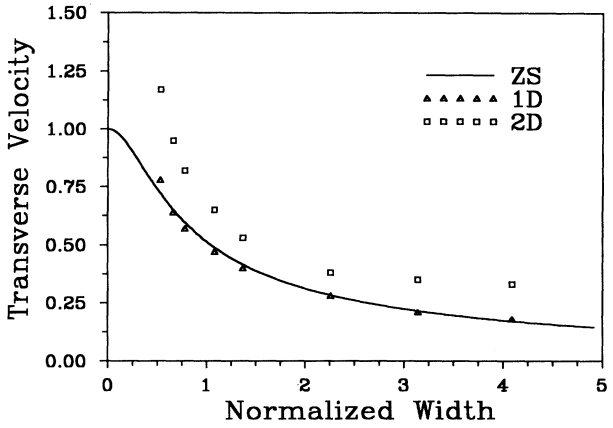

FIG. 7. Comparison between the 1D theory of Zakharov and Shabat (ZS, solid line) [17] and numerically obtained data in 1D (triangles) and 2D (squares).

odd solitons of the same pair generated from an even dark initial condition [17]

$$\lambda_n = 0.5 \tan(\theta) , \tag{7a}$$

and in connection with the normalized width a of the input 1D formation

$$\lambda_n = \cos(2\lambda_n a) . \tag{7b}$$

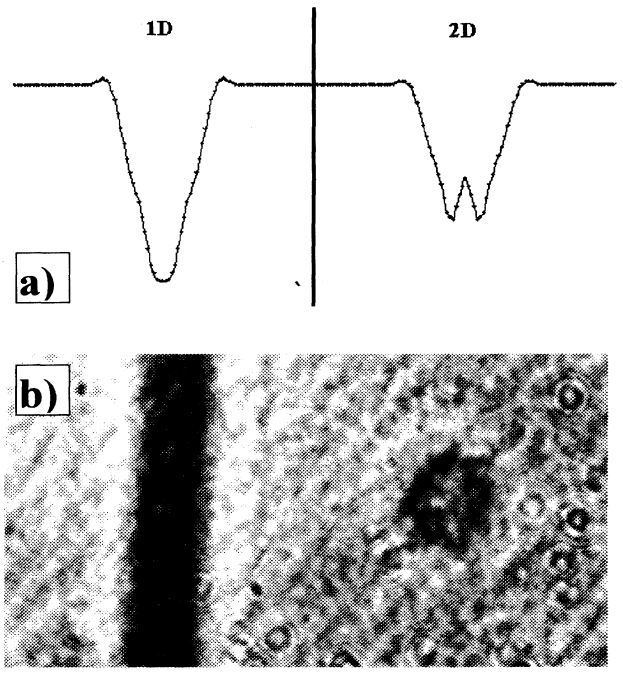

FIG. 8. Numerically generated (a) and experimentally obtained (b) intensity distributions of even 1D and 2D input dark beams, formed by two masks (dot and stripe) with equal transverse dimensions.

In the 2D case, we used the definition of Eq. (7a) with θ being the nonlinear divergence angle of the dark ring.

Figure 6 represents the evolution (obtained from our numerical simulations) of the transverse intensity distribution (as a sequence of radial slices) along the nonlinear medium. A dark beam narrowing prior to the beam splitting is clearly expressed in both the 1D [Fig. 6(a)] and 2D [Fig. 6(b)], as well as the earlier (at shorter nonlinear propagation distance) splitting in the 2D case. Moreover, in the 2D case the transverse velocity λ_n (the divergence angle θ) was found to be higher as compared to the 1D case ($\theta_{2D} > \theta_{1D}$).

The solid curve in Fig. 7 represents the result from the 1D theory of Zakharov and Shabat (ZS) [17] [see Eq. 7(b)]. The triangles denote our numerical results in the 1D case. The slight deviation from the theory at small widths is a result of the computer limited discretization and has no physical meaning. We evaluate the agreement of the numerical results with the theory as more than satisfactory. With squares we plot our results in the 2D case. As seen, the transverse splitting velocity is always higher in the 2D case and, qualitatively, has the same behavior as a function of the normalized width.

Figure 8 presents numerical (the two curves) and experimental (gray-scale image) results demonstrating a formed 2D dark ring without an evident 1D stripe splitting. The 60-μm-sized dot and stripe were positioned on one and the same amplitude mask as close as possible to ensure an equal background intensity, but far enough to prevent a possible interaction.

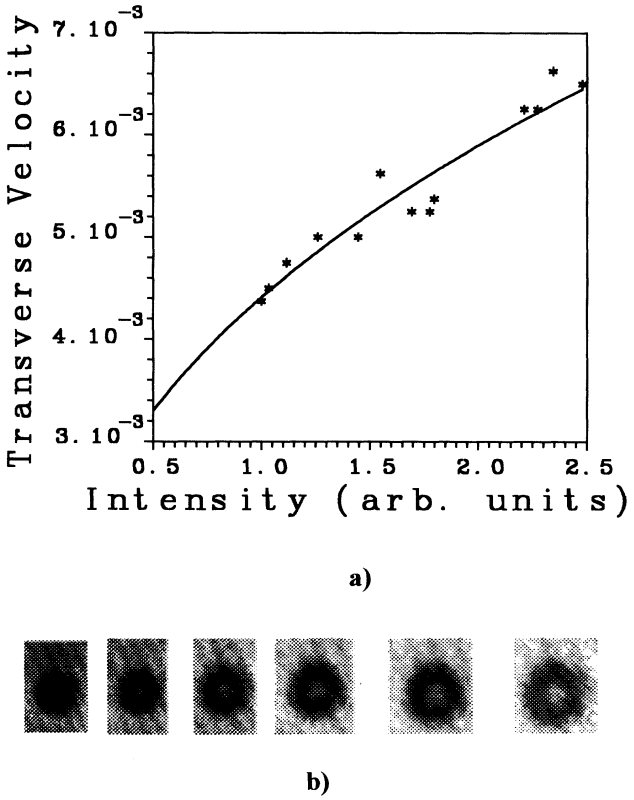

FIG. 9. Dependence of the transverse velocity of the 2D dark soliton ring on the background intensity (a); the first six points are extracted from the experimental pictures shown in (b).

Figure 9(a) plots the intensity dependence of the transverse velocity λ_n at a fixed value of the 2D dark-beam diameter. The dots present the experimental values. The first six of them are extracted from the recorded gray-scale images shown on Fig. 9(b). The solid line corresponds to a power approximation $\lambda_n \sim I^{0.4}$. An analogous numerical experiment yields $\lambda_n \sim I^{0.25}$. Within the experimental inaccuracy of 20% and the numerical inaccuracy due to the limited 2D discretization, the results agree qualitatively well.

In view of the above, we believe we obtained strong evidence for the existence of 2D EDSS (ring dark solitons). Their dynamics and propagation characteristics agree qualitatively with those of the 1D EDSS. The longitudinal (along the nonlinear medium) reduction of the dark ring contrast, however, is a serious difference in comparison to the 1D dark soliton pair.

IV. CONCLUSION

In this paper we demonstrate numerical and experimental results supporting the existence of 2D even and odd dark spatial solitons. The data obtained are fundamentally important since no analytical solutions of the 2D NLSE are known. From a practical point of view, 2D ODSS could be used to form 2D gradient single-mode optical waveguides with nonlinear claddings [8]. Instead from total internal reflection, the spatial guiding effect on the information pulse should result from the induced-phase modulation originating from the 2D ODSS. The experimental results in [9,22] indicate that by using computer-generated holograms, multiple 2D ODSS could be nested in a single background beam. Pure rotational motion of the solitons with respect to the background beam axis could be obtained by changing either the beam intensity or the medium nonlinearity [11]. This experiment is a step toward the realization of an optical rotary switch. The generation of a ring dark soliton from an odd dark soliton described in Sec. II paves the way to redirect radially part of the light guided by the 2D ODSS. The process could be controlled by the background intensity.

Two-dimensional EDSS may appear also to be useful for all-optical manipulation of light. Ring dark solitons could be generated in a controllable way by using computer-generated holograms. The dark ring could guide parallel multiple signal (information) pulses nested in the ring. Initially, they should be separated at suitable axial angles. If the signal (information) beams are of moderate ellipticities, their spatial intensity distribution could be stabilized (i.e., their cross talk could be avoided). The physical mechanisms behind such a signal evolution is the spatial self-phase modulation of elliptical beams assisted by a radial (along the shorter axis of the ellipses) induced-phase modulation. Radial redirection of the information could be achieved by controlling the back-

ground intensity and, therefore, the transverse velocity of the ring. In another possible scheme, an optically induced nonlinear dispersive element [23] could deflect the ring soliton and the signal beams being guided parallely, preserving their mutual ordering. Our results on this problem will be published separately.

The intensity-controllable evolution of both types of 2D dark formations discussed may allow real time reconfiguration [24,25] of nonlinear devices to be achieved.

ACKNOWLEDGMENTS

The authors acknowledge the contribution of D. Tonev during the early stages of the experiments. This work was supported financially by the National Science Fund, Bulgaria, under contract No. F-206.

[1] Yu. Kivshar and X. Yang, Phys. Rev. E **50**, 40 (1994).
[2] Y. Silberg, Opt. Lett. **15**, 1282 (1990).
[3] A. Hasegawa and F. Tappert, Appl. Phys. Lett. **23**, 142 (1973); **23**, 171 (1973).
[4] J. Aitchison, A.Weiner, Y. Silberg, M. Oliver, J. Jackel, D. Leaird, and E. Vogel, Opt. Lett. **15**, 471 (1990).
[5] L. Mollenauer, R. Stolen, and J. Gordon, Phys. Rev. Lett. **45**, 1095 (1980).
[6] J. Aitchison, Y. Silberberg, A. Weiner, D. Leaird, M. Oliver, J. Jackel, E.Vogel, and P. Smith, J. Opt. Soc. Am. B **8**, 1290 (1991).
[7] Yu. Kivshar and X. Yang, Opt. Commun. **107**, 93 (1994).
[8] A. Snyder, L. Poladian, and D. Mithell, Opt. Lett. **17**, 789 (1992).
[9] G. Swartzlander, Jr. and C. Law, Phys. Rev. Lett. **69**, 2503 (1992).
[10] C. Law and G. Swartzlander, Jr., Opt. Lett. **18**, 586 (1993).
[11] B. Luther-Davies, R. Powles, and W. Tikhonenko, Opt. Lett. **15**, 1816 (1994).
[12] P. Coullet, L. Gil, and F. Rocca, Opt. Commun. **73**, 403 (1989).
[13] Yu. Kivshar and X. Yang, Chaos, Solitons Fractals **4**, 1745 (1994).
[14] A. Dreischuh, W. Fliesser, Y. Velchev, S. Dinev, and L. Windholz, Appl. Phys. B (to be published).
[15] D. Andersen, D. Hooton, G. Schwartzlander, Jr., and A. Kaplan, Opt. Lett. **15**, 783 (1990).
[16] G. Schwartzlander, Jr., D. Andersen, J. Regan, H. Yin, and A. Kaplan, Phys. Rev. Lett. **66**, 1583 (1991).
[17] V. Zakharov and A. Shabat, Zh. Éksp. Teor. Fiz. **64**, 1627 (1973) [Sov. Phys. JETP **37**, 823 (1973)].
[18] S. Gredeskul, Yu. Kivshar, and M. Yanovskaya, Phys. Rev. **41**, 3994 (1990).
[19] W. Królikowski, N. Akhmediev, and B. Luther-Davies, Phys. Rev. E **48**, 3980 (1993).
[20] W. Tomlinson, R. Hawkins, A. Weiner, J. Heritage, and R. Thurston, J. Opt. Soc. Am. B **6**, 329 (1989).
[21] G. P. Agrawal, *Nonlinear Fiber Optics* (Academic, Boston, 1989).
[22] B. Luther-Davis and X. Yang, Opt. Lett. **17**, 1755 (1992).
[23] Y. Li, D. Chen, and R. Alfano, Opt. Lett. **16**, 438 (1991).
[24] A. Cruz-Cabrera and S. Skinner, Opt. Lett. **18**, 1403 (1993).
[25] R. Jin, M. Liang, G. Khitrova, H. Gibbs, and N. Peyghambarian, Opt. Lett. **18**, 404 (1993).

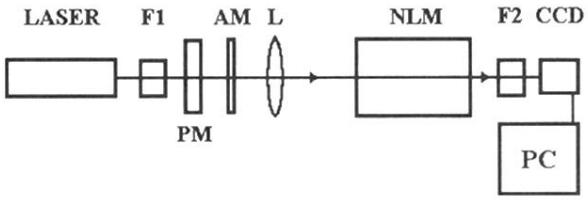

a)

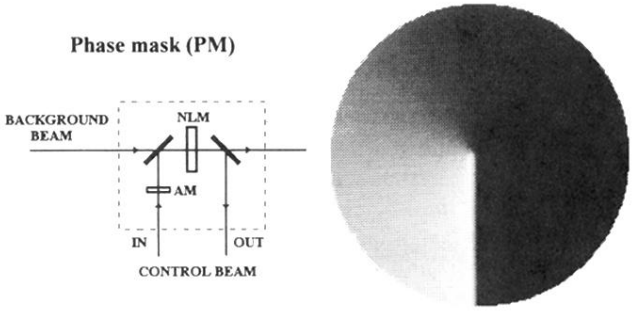

b)

FIG. 2. (a) Experimental scheme, corresponding to the numerical simulations. ($F1$, $F2$ are the filter sets; NLM is the self-defocusing nonlinear medium; AM is the amplitude mask for obtaining a 2D dip on the background; CCD denotes the camera and PC is the personal computer.) The PM should generate the desired radial π jump. (b) Possible scheme for achieving the appropriate background phase distribution. NLM denotes the thin nonlinear medium; the amplitude mask (AM) transmission (gray-scale coded) is plotted too.

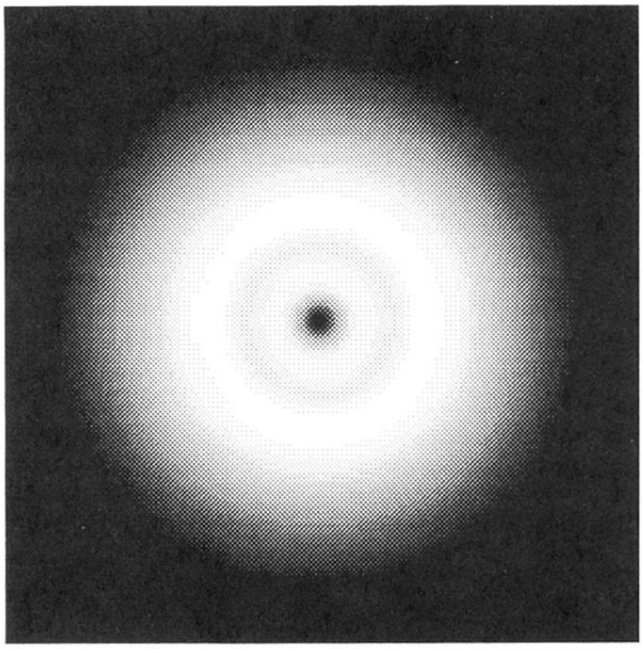

a)

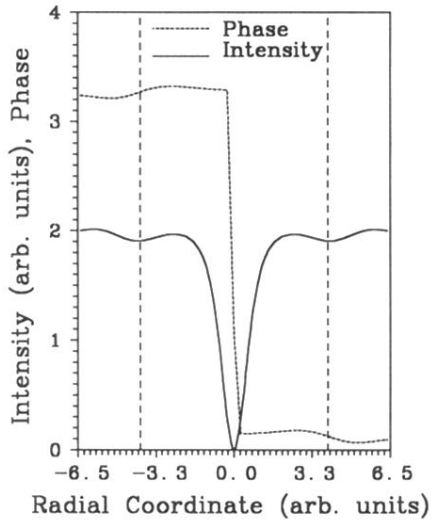

(b)

FIG. 4. Gray-scale image of the output 2D odd dark formation with $A_0 = 2.1$ at $Z = 10L_{nl}$ (a) and the corresponding radial intensity and phase distributions (b).

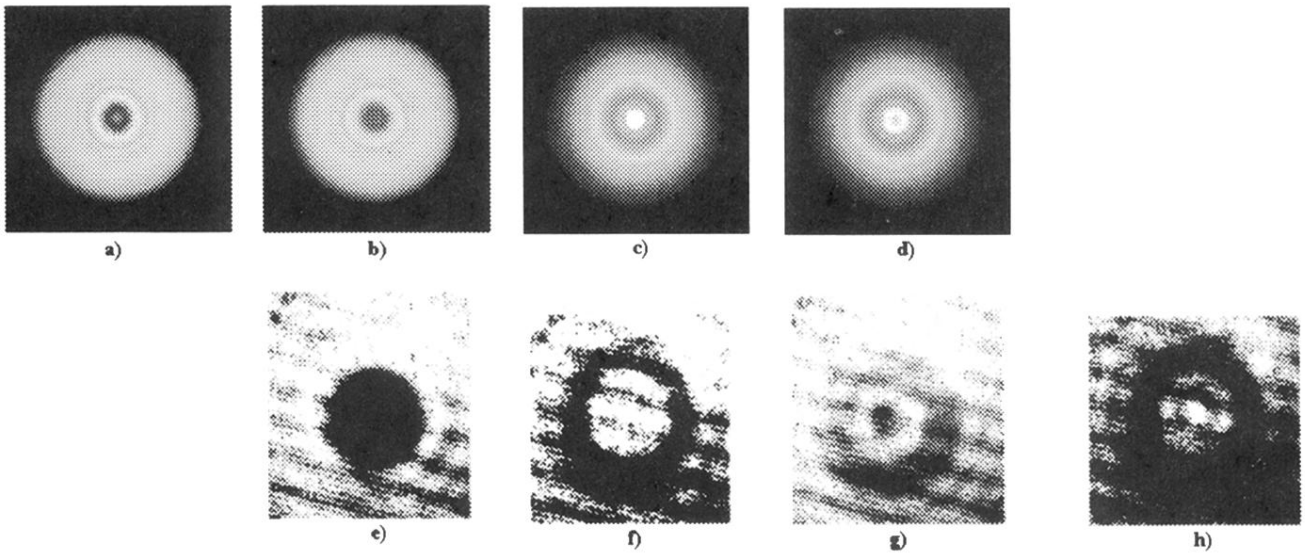

FIG. 5. Characteristic evolution stages of a 2D EDSS [(a)–(d) are numerically simulated; (e)–(h) are experimentally obtained]: Poisson spot at dark-beam center (a); diffraction compensated by the nonlinearity (b) and (e); first dark soliton ring (c) and (f); initial stage of the second dark soliton ring formation (d) and (g); two dark soliton rings (h).

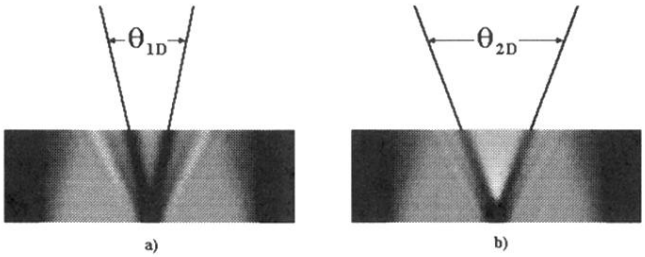

FIG. 6. Evolution of the transverse intensity distribution (as a sequence of radial slices) along the nonlinear medium. (a) 1D case; (b) 2D case.

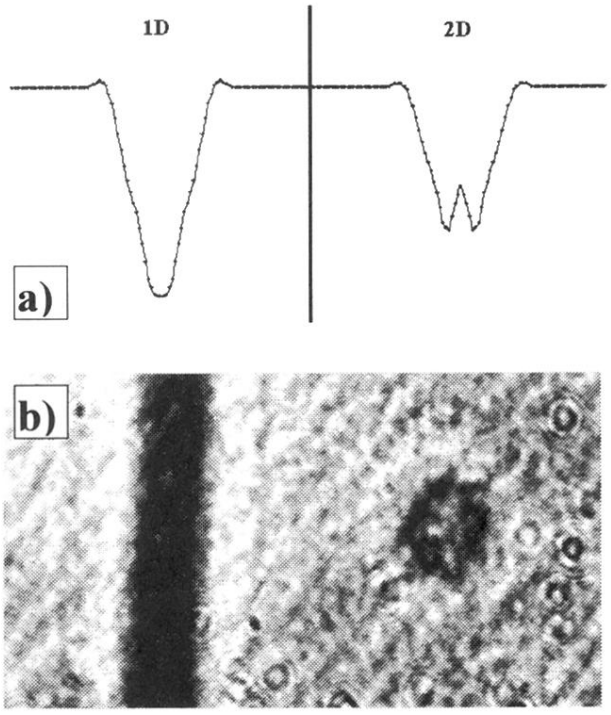

FIG. 8. Numerically generated (a) and experimentally obtained (b) intensity distributions of even 1D and 2D input dark beams, formed by two masks (dot and stripe) with equal transverse dimensions.

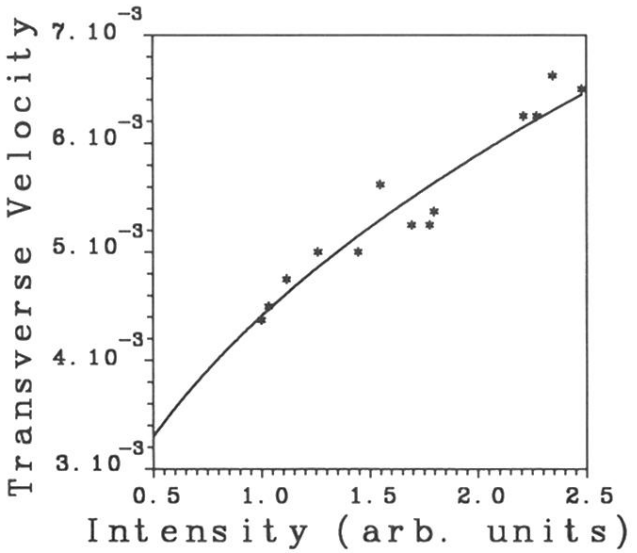

a)

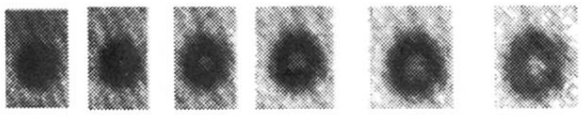

b)

FIG. 9. Dependence of the transverse velocity of the 2D dark soliton ring on the background intensity (a); the first six points are extracted from the experimental pictures shown in (b).